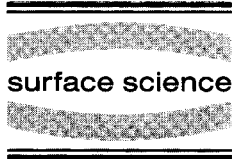




ELSEVIER

Surface Science 366 (1996) 377–393



surface science

# Statistical multiple diffuse scattering from rough surfaces in RHEED – beyond the distorted-wave Born approximation

Z.L. Wang \*

*School of Material Science and Engineering, Georgia Institute of Technology, Atlanta, GA 30332-0245, USA*

Received 25 January 1996; accepted for publication 8 May 1996

---

## Abstract

In reflection high-energy electron diffraction (RHEED) of growing surfaces in molecular beam epitaxy (MBE), diffuse scattering is generated by atom vibrations, point vacancies and growth islands (or surface roughness). Most of the existing RHEED theories have been developed under the first-order diffuse scattering approximation, and thus they are restricted for surfaces whose roughness is relatively low. In fact, crystal surfaces grown by MBE are usually rough; the change of surface coverage from 0 to 1 monolayer accounts for the observed RHEED oscillation. In this paper, a formal dynamical theory of RHEED has been developed to calculate the diffuse scattering produced by both atom vibrations and point vacancies at surfaces. The theory is aimed at recovering the multiple diffuse scattering that has been dropped by the distorted-wave Born approximation (DWBA). With the inclusion of a complex potential in the dynamical calculation, a rigorous proof is given to show that the high-order diffuse scattering terms are recovered in the calculation using the equation originally derived under the DWBA. This conclusion establishes the basis for expanding the RHEED theories developed under the first-order diffuse scattering to cases where the degree of surface roughness is high, allowing dynamical calculation of RHEED rocking curves for any growing surface. The statistical time and structure averages over the distorted crystal potential are evaluated analytically before numerical calculation. The dynamic form factor is calculated with consideration of anisotropic surface atom vibration and point vacancies at a growing surface.

*Keywords:* Distorted wave-born approximation; Point defect; Reflection high-energy electron diffraction (RHEED); Surface range order; Surface roughness; Thermal diffuse scattering

---

## 1. Introduction

Reflection high-energy electron diffraction (RHEED) is a powerful technique for in-situ observation of surface structural evolution during molecular beam epitaxial (MBE) growth. RHEED oscillation is a sensitive technique for monitoring layer-by-layer growth on crystalline surfaces. RHEED has been routinely used to monitor the growth of surface layers, and it has been demon-

strated to exhibit high surface sensitivity because the electron penetration depth into the surface is no more than 1–2 nm. Surface structures can now be determined quantitatively using RHEED, in which dynamical calculation plays an essential role [1–3].

There are three types of elastic scattering theories which have been proposed for RHEED calculations. The Bloch wave theory developed by Bethe [4] for transmission electron diffraction was first applied in RHEED by Colella [5] and Moon [6]. In this theory, the crystal is considered as a periodic repetition of a unit cell, and the surface is a sharp

---

\* Corresponding author. Fax: +1 404 8949140;  
e-mail: zhong.wang@mse.gatech.edu

cut-off of the crystal. The Bloch waves are the eigen solutions of the Schrödinger equation, analogous to the case for transmission electron diffraction. This theory is unable to take into account any irregular surface structures, such as defects, the tail of surface potential, and surface relaxation. To incorporate surface potential effects and surface relaxation in RHEED calculations, other multi-slice approaches have been proposed in which a crystal is considered periodic in the plane parallel to the surface, and non-periodic modulations of the potential only occur in the direction normal to the surface [7–14]. The crystal

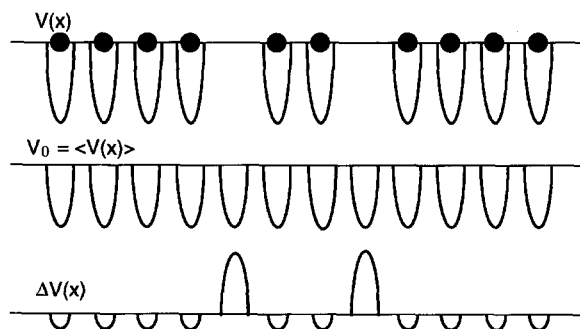


Fig. 1. One-dimensional representation of crystal potential  $V$ , the structurally averaged potential  $V_0 = \langle V \rangle$  and the deviation potential  $\Delta V = V - V_0$ .  $V_0$  is a periodic function but  $\Delta V$  is not. Solid circles represent atoms.

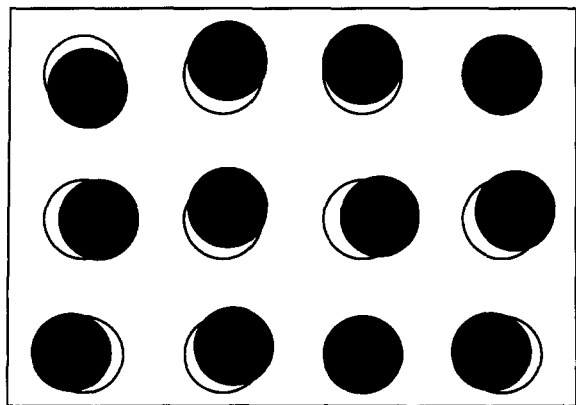


Fig. 2. Schematic diagram showing instantaneous crystal lattices due to thermal vibration. Solid circles are the atoms, open circles are their equilibrium positions. Each configuration is considered as a “static” lattice in the theoretical calculation, and the observed intensity is a statistical time average of the intensities contributed by all possible lattice configurations.

is sliced parallel to the surface plane and the reflected waves are calculated slice-by-slice from the last slice. These are the parallel-to-surface multi-slice theories. The last approach uses the multi-slice theory originally developed for transmission electron scattering in a thin crystal. The theory has been adopted for RHEED calculation if the slice is cut normal to the surface and the electron beam azimuth [15]. The crystal and the vacuum parts, in which the incident beam approaches the surface, are defined as a super-cell. The entire space is filled with the repetition of the super-cell. The slice is partly filled with atoms, and the other part is a vacuum. The transmitted waves inside the crystal and the reflected waves in the vacuum are calculated simultaneously.

These theories have been developed for calculating the elastic scattering behavior of the incident electron in RHEED geometry (for a review, see Ref. [16]). In practice, the interaction between an incident electron and the atoms in condensed matter results in various inelastic scattering processes (for a review, see Ref. [17]). Thermal diffuse scattering (TDS) or phonon scattering is the result of atomic vibrations in crystals. This process does not introduce any significant energy loss ( $<0.1$  eV), smaller than the energy spread of the electron emission source, but produces large momentum transfer. Valence loss (or plasmon for metals and semiconductors) excitation, which characterizes the transitions of electrons from the valence band to the conduction band, involves an energy loss in the range 1–50 eV. This inelastic scattering process is particularly important in RHEED because more than 50–90% of the electrons have lost the energy of plasmons due to the long-range interaction of the electron with the specimen [16]. Atomic inner-shell ionization is excited by the energy transfer of the incident electron, resulting in an ejected electron from a deep-core state. This process is a signature of the corresponding element, and thus it can be used to determine the specimen chemical composition. In addition to these characteristic energy-loss processes, continuous energy-loss spectra can be generated by an electron which penetrates into the specimen and undergoes collisions with the atoms in it. The electromagnetic radiation produced is known as “Bremsstrahlung”,

leading to continuous energy loss that increases with increasing scattering angle. X-rays are usually generated. The other continuous process is the energy transfer due to collision of the incident electron with an electron belonging to the specimen. This process is known as “electron Compton scattering” or “electron–electron (e–e) scattering”. All of these processes make a contribution to the RHEED pattern.

Recent progress in instrumentation has made it possible to filter away the contribution in the RHEED patterns made by electrons that have suffered energy losses larger than a few eV [18–20], but the TDS electrons remain. If one only considers the Bragg reflections, TDS is equivalent to introduce an absorption function in the elastic calculation, but the thermal diffusely scattered electrons still remain in the diffraction pattern, and are distributed in the angular ranges between Bragg beams. Inclusion of TDS in dynamical calculation has a long history; substantial research was performed when the dynamical theory for low-energy electron diffraction (LEED) was developed [21–26]. The theory was even able to cover multiple elastic scattering before and after inelastic scattering [26,27]. In RHEED of growing surfaces in MBE, in addition to TDS, distorted surface structure plays a vital role in producing diffuse scattering, and various theoretical approaches have been developed to calculate the diffuse scattering patterns [28–33] in order to quantify the RHEED oscillation curves [34]. These theories are essentially based on the first-order perturbation theory, in which only the  $\Delta V^2$  term is considered in dynamical calculation. This approximation is equivalent to the distorted-wave Born approximation (DWBA) [35] used in LEED calculations [26,27], which holds if the distorted potential is much smaller than the crystal potential. However, in RHEED of growing surfaces, the surface coverage changes from 0 to 1 and the surface can be very rough, so that the distorted potential is compatible to the crystal potential. It is therefore essential to develop a dynamical theory which can be applied to cases where the surface is very rough. This is the objective of the current paper.

In this paper, we first outline a general approach

for calculating diffuse scattering under the DWBA. Then, this theory is modified to include the high-order diffuse scattering terms by introducing a complex potential in the calculation of the elastic wave (Section 2). A rigorous proof is given to show that this approach does work, making it possible to expand the existing RHEED theories accounting for the high-order diffuse scattering. Then, details are given for calculating RHEED intensity (Section 3). In Section 4, applications of this general approach for RHEED are presented in the schemes of Bloch wave theory and the parallel-to-surface multi-slice theory. Then, the dynamic form factors are derived for describing thermal diffuse scattering, including anisotropic atom vibration behavior and point defect scattering (Section 5).

## 2. A multiple diffuse scattering theory

To include the effect of point vacancies and TDS in RHEED calculation, one uses a general approach in which an average crystal structure is introduced [31,36,37]. The crystal potential  $V(\mathbf{r},t)$  is written in the form

$$V(\mathbf{r},t) = V_0(\mathbf{r}) + \Delta V(\mathbf{r},t), \quad (1)$$

where  $V_0(\mathbf{r}) = \langle V(\mathbf{r},t) \rangle_{ts}$  is the crystal potential distribution function for the average lattice, defined to be time-independent and periodic,  $\langle \rangle_{ts}$  indicates the statistical time and structure average, and  $\Delta V(\mathbf{r})$  represents the deviation from the average lattice, which is non-periodic and time-dependent (for TDS). This distorted wave approach is shown schematically in Fig. 1 for a one-dimensional point vacancy case. The statistical structure average takes into account the point vacancies distributed in the bulk and surface lattices.

In high-energy electron scattering, since the interaction time between an incident electron with the specimen is much shorter than the vibration period of the atom, the crystal atoms are seen as if stationary by the incident electron. This is the “frozen” lattice model which has been used to treat TDS, as shown schematically in Fig. 2. The main task involved in the theory is to perform the statistical time average over the electron diffraction

intensities for a vast number of different thermal vibration configurations. The first objective in this theory is to find the scattered electron wave for a given frozen lattice configuration. We start from the time-independent Schrödinger equation with relativistic correction

$$\left(-\frac{\hbar^2}{2m_0}\nabla^2 - e\gamma V_0 - e\gamma\Delta V - E\right)\Psi = 0. \quad (2)$$

where  $E = eU_0[1 + (eU_0/2m_0c^2)]$ ,  $U_0$  is the accelerating voltage of the electron gun, the relativistic factor  $\gamma = (1 - v^2/c^2)^{-1/2}$ , and  $v$  is the electron velocity. Eq. (2) can be converted into an integral equation with the use of the Green's function

$$\Psi(\mathbf{r}, t) = \Psi_0(\mathbf{K}_0, \mathbf{r}) + \int d\mathbf{r}_1 G(\mathbf{r}, \mathbf{r}_1)[e\gamma\Delta V(\mathbf{r}_1, t)\Psi(\mathbf{r}_1, t)], \quad (3)$$

where  $G$  is the Green's function satisfying

$$\left(-\frac{\hbar^2}{2m_0}\nabla^2 - e\gamma V_0 - E\right)G(\mathbf{r}, \mathbf{r}_1) = \delta(\mathbf{r} - \mathbf{r}_1), \quad (4)$$

and  $\Psi_0(\mathbf{K}_0, \mathbf{r})$  is the elastic wave scattered by the periodic, time-independent average potential  $V_0$  due to an incident plane wave with wave vector  $\mathbf{K}_0$ , which satisfies

$$\left(-\frac{\hbar^2}{2m_0}\nabla^2 - e\gamma V_0 - E\right)\Psi_0 = 0. \quad (5)$$

Eq. (3) can be solved iteratively, but the convergence of the series depends on the relative magnitude of  $\Delta V$  with respect to  $V_0$ . The most common approximation adopted in the literature [21–33] is the DWBA, in which  $\Psi$  is replaced by  $\Psi_0$ , equivalent to the first-order diffuse scattering approximation. Thus Eq. (3) is approximated as

$$\Psi(\mathbf{r}, t) \approx \Psi_0(\mathbf{K}_0, \mathbf{r}) + \int d\mathbf{r}_1 G(\mathbf{r}, \mathbf{r}_1)[e\gamma\Delta V(\mathbf{r}_1, t)\Psi_0(\mathbf{r}_1, t)]. \quad (6)$$

This equation holds if the disorder of the surface is low, so that  $|\Delta V| \ll V_0$ . For a growing surface in RHEED, however, the surface roughness can be very high and this approximation fails in most cases. It is thus necessary to develop a theory which can recover the high-order diffuse scattering terms dropped by the DWBA. This is the focal point of the following approach.

To compensate the dropped high-order diffuse scattering terms in Eq. (6), a complex potential  $V$  is added in Eq. (5)

$$\left(-\frac{\hbar^2}{2m_0}\nabla^2 - e\gamma V_0 - e\gamma V' - E\right)\Psi_0 = 0, \quad (7)$$

and  $V$  is chosen in such a way that the wave function  $\Psi_0$  determined by Eq. (6) is the exact solution of Eq. (2). The high-order diffuse scattering beyond the DWBA can be recovered if a unique solution of  $V$  can be found. This is the main idea behind this method. Substituting Eqs. (6) into (2) and using Eq. (7),  $V$  is required to satisfy (see Appendix A)

$$[V'\Psi_0] = e\gamma \int d\mathbf{r}_1 [G(\mathbf{r}, \mathbf{r}_1)\Delta V(\mathbf{r}, t)\Delta V(\mathbf{r}_1, t)\Psi_0(\mathbf{K}_0, \mathbf{r}_1)]. \quad (8)$$

It is apparent that  $V$  is a non-local function and it has the exact form as the optical potential introduced in elastic scattering to cover the effects arising from inelastic scattering [38–40]. Before we proceed, the first objective is to prove that the optical potential  $V$  given by Eq. (8) can be applied to recover the high-order diffuse scattering terms dropped when  $\Psi(\mathbf{r}_1, t)$  is replaced by  $\Psi_0(\mathbf{K}_0, \mathbf{r}_1)$  in deriving Eq. (6). Starting from the integral form of Eq. (7) with the use of Green's function and iterative calculation, the elastic wave is expanded as

$$\begin{aligned} \Psi_0(\mathbf{r}, t) &= \Psi_0^{(0)}(\mathbf{K}_0, \mathbf{r}) + e\gamma \int d\mathbf{r}_1 \\ &\quad \times G(\mathbf{r}, \mathbf{r}_1)[V'(\mathbf{r}_1)\Psi_0(\mathbf{K}_0, \mathbf{r}_1)] \\ &= \Psi_0^{(0)}(\mathbf{K}_0, \mathbf{r}) + (e\gamma)^2 \int d\mathbf{r}_1 G(\mathbf{r}, \mathbf{r}_1) \\ &\quad \int d\mathbf{r}_2 [G(\mathbf{r}_1, \mathbf{r}_2)\Delta V(\mathbf{r}_1, t)\Delta V(\mathbf{r}_2, t)\Psi_0(\mathbf{K}_0, \mathbf{r}_2)] \\ &= \Psi_0^{(0)}(\mathbf{K}_0, \mathbf{r}) + (e\gamma)^2 \int d\mathbf{r}_1 \int d\mathbf{r}_2 G(\mathbf{r}, \mathbf{r}_1) \\ &\quad \times G(\mathbf{r}_1, \mathbf{r}_2)\Delta V(\mathbf{r}_1, t)\Delta V(\mathbf{r}_2, t)\Psi_0^{(0)}(\mathbf{K}_0, \mathbf{r}_2) \\ &\quad + (e\gamma)^4 \int d\mathbf{r}_1 \int d\mathbf{r}_2 \int d\mathbf{r}_3 \int d\mathbf{r}_4 G(\mathbf{r}, \mathbf{r}_1) \\ &\quad \times G(\mathbf{r}_1, \mathbf{r}_2)G(\mathbf{r}_2, \mathbf{r}_3)G(\mathbf{r}_3, \mathbf{r}_4)\Delta V(\mathbf{r}_1, t)\Delta V(\mathbf{r}_2, t) \\ &\quad \times \Delta V(\mathbf{r}_3, t)\Delta V(\mathbf{r}_4, t)\Psi_0^{(0)}(\mathbf{K}_0, \mathbf{r}_4) + \dots \end{aligned} \quad (9)$$

where  $\Psi_0^{(0)}$  is the Bragg scattered wave due to the average periodic lattice at the absence of  $V$  (e.g.

no absorption)

$$\left(-\frac{\hbar^2}{2m_0}\nabla^2 - e\gamma V_0 - E\right)\Psi_0^{(0)} = 0. \quad (10)$$

This equation can be solved using conventional dynamic electron diffraction theory [4–15]. Substituting Eq. (9) into Eq. (6), the total scattered wave is

$$\begin{aligned} \Psi(\mathbf{r}, t) = & \Psi_0^{(0)}(\mathbf{K}_0, \mathbf{r}) + (e\gamma) \int d\mathbf{r}_1 \\ & \times G(\mathbf{r}, \mathbf{r}_1) \Delta V(\mathbf{r}_1, t) \Psi_0^{(0)}(\mathbf{K}_0, \mathbf{r}_1) \\ & + (e\gamma)^2 \int d\mathbf{r}_1 \int d\mathbf{r}_2 G(\mathbf{r}, \mathbf{r}_1) \\ & \times G(\mathbf{r}_1, \mathbf{r}_2) \Delta V(\mathbf{r}_1, t) \Delta V(\mathbf{r}_2, t) \Psi_0^{(0)}(\mathbf{K}_0, \mathbf{r}_2) \\ & + (e\gamma)^3 \int d\mathbf{r}_1 \int d\mathbf{r}_2 \int d\mathbf{r}_3 G(\mathbf{r}, \mathbf{r}_1) G(\mathbf{r}_1, \mathbf{r}_2) \\ & \times G(\mathbf{r}_2, \mathbf{r}_3) \Delta V(\mathbf{r}_1, t) \Delta V(\mathbf{r}_2, t) \Delta V(\mathbf{r}_3, t) \Psi_0^{(0)}(\mathbf{K}_0, \mathbf{r}_3) \\ & + (e\gamma)^4 \int d\mathbf{r}_1 \int d\mathbf{r}_2 \int d\mathbf{r}_3 \int d\mathbf{r}_4 G(\mathbf{r}, \mathbf{r}_1) G(\mathbf{r}_1, \mathbf{r}_2) \\ & \times G(\mathbf{r}_2, \mathbf{r}_3) G(\mathbf{r}_3, \mathbf{r}_4) \Delta V(\mathbf{r}_1, t) \Delta V(\mathbf{r}_2, t) \\ & \times \Delta V(\mathbf{r}_3, t) \Delta V(\mathbf{r}_4, t) \Psi_0^{(0)}(\mathbf{K}_0, \mathbf{r}_4) + \dots \end{aligned} \quad (11)$$

This equation is the exact iterative solution of Eq. (2). The third term in Eq. (11) is taken as an example to show its physical meaning. The Bragg scattered wave is diffusely scattered at  $\mathbf{r}_2$  by  $\Delta V(\mathbf{r}_2, t)$ . The diffusely scattered wave is elastically scattered by the crystal lattice while propagating from  $\mathbf{r}_2$  to  $\mathbf{r}_1$  [ $G(\mathbf{r}_1, \mathbf{r}_2)$ ], then second-order diffuse scattering occurs at  $\mathbf{r}_1$  ( $\Delta V(\mathbf{r}_1, t)$ ). Finally, the double diffusely scattered wave exits the crystal at  $\mathbf{r}$  after elastic scattering when propagating from  $\mathbf{r}_1$  to  $\mathbf{r}$  [ $G(\mathbf{r}, \mathbf{r}_1)$ ]. The integrals over  $\mathbf{r}_1$  and  $\mathbf{r}_2$  are to sum over the contributions made by all the possible scattering sources in the crystal.

Therefore, the multiple diffusely scattered waves are comprehensively included in the calculation of Eq. (6) if the optical potential  $V$  given by Eq. (8) is introduced in the calculation of  $\Psi_0$  [Eq. (7)]. This is a key conclusion which means that, by introducing a proper form of the optical potential, the multiple diffuse scattering terms are automatically included in the calculation using Eq. (6), although it was derived under the DWBA. This result establishes the basis for expanding the existing diffuse RHEED theories developed under the DWBA to a surface with a high degree of disorder.

This conclusion can be phenomenologically understood as follows. The optical potential first introduced by Yoshioka [39] was to include the effect of inelastic scattering on the elastic scattering. If the transition from the elastic state to an inelastic state is denoted by a transition matrix  $H_{n0}$ , the transition from the inelastic state to the elastic state is  $H_{0n}$ , which equals  $[H_{n0}]^*$ . This simply means that the optical potential has a register relation with the inelastic scattering and it “knows” the nature of the inelastic excitation. If we can use this potential to correct the “absorption” effect produced by the inelastic scattering, the potential can be applied inversely to retrieve the inelastic scattering component. Since there is no energy loss associated with diffuse scattering, the retrieval of high-order diffuse scattering terms by  $V$  is adequate, as proved rigorously in the approach described above.

If the Green’s function is replaced by its form in free space, the approximation adopted by Yoshioka [39]

$$G_0(\mathbf{r}, \mathbf{r}_1) = \frac{2m_0}{\hbar^2} \frac{\exp(2\pi i K_0 |\mathbf{r} - \mathbf{r}_1|)}{4\pi |\mathbf{r} - \mathbf{r}_1|}, \quad (12)$$

Eq. (11) is approximated to include all of the orders of diffuse scattering except the dynamical Bragg diffraction after each diffuse scattering. In this paper, this approximation is *not* assumed.

### 3. Multiple diffuse scattering in RHEED calculation

In RHEED, the observation point is considered at infinity with respect to the interaction region of the beam with the specimen. The coordinate system used for the following analysis is shown in Fig. 3, where the incident beam is nearly parallel to  $z$ -axis and the  $x$ -axis is inward perpendicular to the surface. The observed RHEED pattern is the modulus square of the two-dimensional Fourier transform (FT) of  $\Psi(\mathbf{r})$ ,

$$\begin{aligned} I(\mathbf{u}_b) = & \langle |\text{FT}[\Psi(x, y, \infty)]|^2 \rangle \\ = & \langle |\Phi_0(\mathbf{K}_0, \mathbf{u}_b, t) + \int d\mathbf{r}_1 \hat{G}(\mathbf{u}_b, \mathbf{r}_1) \\ & \times [e\gamma \Delta V(\mathbf{r}_1, t) \Psi(\mathbf{r}_1, t)]|^2 \rangle_{\text{ts}}, \end{aligned} \quad (13)$$

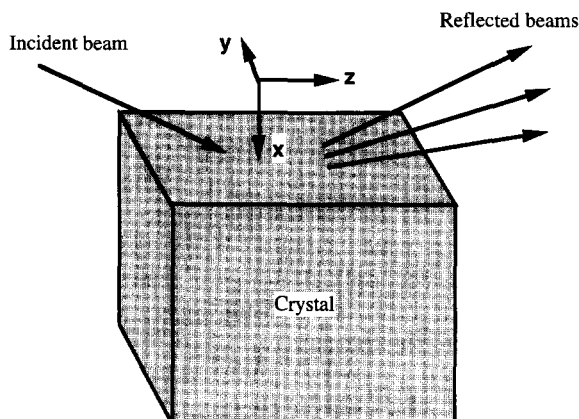


Fig. 3. The coordinate system used in RHEED theory. The incident beam is nearly parallel to the  $z$ -axis, and the  $x$ -axis is perpendicular to the crystal surface inward.

where  $\mathbf{u}_b = (u_x, u_y)$  is a two-dimensional reciprocal vector perpendicular to the incident beam direction,  $\Phi_0(\mathbf{K}_0, \mathbf{u}_b, t) = \text{FT}[\Psi_0(\mathbf{K}_0, x, y, \infty)]$  and  $\hat{G}(\mathbf{u}_b, \mathbf{r}_1) = \text{FT}[G(x, y, z = \infty, \mathbf{r}_1)]$ . The statistical time and structure averages are added to obtain the contribution made by various lattice configuration of the distorted structure. In this section, we first outline the theory for calculating the intensity of multiple diffusely scattered electrons using the theoretical scheme described in Section 2. The expansion of Eq. (13) gives four terms

$$\begin{aligned}
 I(\mathbf{u}_b) &= \langle |\Phi_0(\mathbf{K}_0, \mathbf{u}_b, t)|^2 \rangle_{ts} + e\gamma \int d\mathbf{r}_1 \hat{G}(\mathbf{u}_b, \mathbf{r}_1) \\
 &\quad \times \langle [\Phi_0^*(\mathbf{K}_0, \mathbf{u}_b, t) \Delta V(\mathbf{r}_1, t) \Psi_0(\mathbf{r}_1, t)] \rangle_{ts} \\
 &\quad + e\gamma \int d\mathbf{r}_1 \hat{G}^*(\mathbf{u}_b, \mathbf{r}_1) \\
 &\quad \times \langle [\Phi_0(\mathbf{K}_0, \mathbf{u}_b, t) \Delta V(\mathbf{r}_1, t) \Psi_0^*(\mathbf{r}_1, t)] \rangle_{ts} \\
 &\quad + (e\gamma)^2 \int d\mathbf{r}_1 \int d\mathbf{r}_2 \hat{G}(\mathbf{u}_b, \mathbf{r}_1) \hat{G}^*(\mathbf{u}_b, \mathbf{r}_2) \\
 &\quad \times \langle \Delta V(\mathbf{r}_1, t) \Delta V(\mathbf{r}_2, t) \Psi_0(\mathbf{r}_1, t) \Psi_0^*(\mathbf{r}_2, t) \rangle_{ts}. \quad (14)
 \end{aligned}$$

From the definition of the distorted potential  $\Delta V$ ,  $\langle \Delta V \rangle_{ts} = 0$ , thus, the average of the odd order terms of  $\Delta V$  approximately vanish, e.g.  $\langle \Delta V^3 \rangle_{ts} \approx 0$ ,  $\langle \Delta V^5 \rangle_{ts} \approx 0$  etc. This means that some of the interference terms between different orders of diffuse scattering are treated as incoherent. This is an excellent approximation, and no scattering intensity is dropped (see Appendix B for proof). Also consider the fact that the expansion of

$\Psi_0(\mathbf{r}_1, t)$  contains only even order terms of  $\Delta V$  (i.e.  $\Delta V^2, \Delta V^4$  etc.) (see Eq. (9)), the second and the third terms (which are the cross terms of the Bragg reflections with the diffuse scattering) in Eq. (14) approximately vanish

$$\begin{aligned}
 I(\mathbf{u}_b) &\approx \langle |\Phi_0(\mathbf{K}_0, \mathbf{u}_b, t)|^2 \rangle_{ts} \\
 &\quad + (e\gamma)^2 \int d\mathbf{r}_1 \int d\mathbf{r}_2 \hat{G}(\mathbf{u}_b, \mathbf{r}_1) \\
 &\quad \times \hat{G}^*(\mathbf{u}_b, \mathbf{r}_2) \langle \Delta V(\mathbf{r}_1, t) \Delta V(\mathbf{r}_2, t) \\
 &\quad \times \Psi_0(\mathbf{r}_1, t) \Psi_0^*(\mathbf{r}_2, t) \rangle_{ts}. \quad (15)
 \end{aligned}$$

Consider the fact that the expansion of  $\Psi_0(\mathbf{r}_1, t)$  contains only even orders of  $\Delta V$  terms. We can split the average by an approximation of

$$\begin{aligned}
 \langle \Delta V^4 \rangle_{ts} &\approx \langle \Delta V^2 \rangle_{ts} \langle \Delta V^2 \rangle_{ts}, \\
 \langle \Delta V^6 \rangle_{ts} &\approx \langle \Delta V^2 \rangle_{ts} \langle \Delta V^2 \rangle_{ts} \langle \Delta V^2 \rangle_{ts}, \\
 \text{etc.}, \quad (16a)
 \end{aligned}$$

and

$$\begin{aligned}
 &\langle \Delta V(\mathbf{r}_1, t) \Delta V(\mathbf{r}_2, t) \Psi_0(\mathbf{r}_1, t) \Psi_0^*(\mathbf{r}_2, t) \rangle_{ts} \\
 &\approx \langle \Delta V(\mathbf{r}_1, t) \Delta V(\mathbf{r}_2, t) \rangle_{ts} \langle \Psi_0(\mathbf{r}_1, t) \Psi_0^*(\mathbf{r}_2, t) \rangle_{ts}.
 \end{aligned}$$

Hence,

$$\langle |\Phi_0(\mathbf{K}_0, \mathbf{u}_b, t)| \rangle_{ts} \approx |\langle \Phi_0(\mathbf{K}_0, \mathbf{u}_b, t) \rangle_{ts}|^2, \quad (16b)$$

where  $\langle \Phi_0(\mathbf{K}_0, \mathbf{u}_b, t) \rangle_{ts}$  is the 2D Fourier transform of  $\langle \Psi_0(\mathbf{K}_0, \mathbf{r}) \rangle_{ts}$  at  $z = \infty$ , satisfying

$$\begin{aligned}
 &\left( -\frac{\hbar^2}{2m_0} \nabla^2 - e\gamma V_0 - E \right) \langle \Psi_0 \rangle_{ts} \\
 &= (e\gamma)^2 \int d\mathbf{r}_1 [G(\mathbf{r}, \mathbf{r}_1) \langle \Delta V(\mathbf{r}, t) \\
 &\quad \times \Delta V(\mathbf{r}_1, t) \rangle_{ts} \langle \Psi_0(\mathbf{K}_0, \mathbf{r}_1) \rangle_{ts}. \quad (17)
 \end{aligned}$$

The approximation made in Eq. (16a) does not produce any significant error, a rigorous proof shows (see Appendix B) that the entire scattering intensity is preserved. The theory for solving Eq. (17) is given in Section 4. The diffracted intensity is

$$\begin{aligned}
 I(\mathbf{u}_b) &\approx |\langle \Phi_0(\mathbf{K}_0, \mathbf{u}_b, t) \rangle_{ts}|^2 \\
 &\quad + (e\gamma)^2 \int d\mathbf{r}_1 \int d\mathbf{r}_2 \hat{G}(\mathbf{u}_b, \mathbf{r}_1) \\
 &\quad \times \hat{G}^*(\mathbf{u}_b, \mathbf{r}_2) \langle \Delta V(\mathbf{r}_1, t) \Delta V(\mathbf{r}_2, t) \rangle_{ts} \\
 &\quad \times \langle \Psi_0(\mathbf{r}_1, t) \rangle_{ts} \langle \Psi_0^*(\mathbf{r}_2, t) \rangle_{ts}, \quad (18)
 \end{aligned}$$

and the following expansions are provided to illustrate the physical meaning of Eq. (18)

$$\begin{aligned} \langle \Phi_0(\mathbf{K}_0, \mathbf{u}_b, t) \rangle_{ts} &= \Phi_0^{(0)}(\mathbf{K}_0, \mathbf{u}_b) + (e\gamma)^2 \int d\mathbf{r}_1 \int d\mathbf{r}_2 \\ &\times \hat{G}(\mathbf{u}_b, \mathbf{r}_1) G(\mathbf{r}_1, \mathbf{r}_2) \langle \Delta V(\mathbf{r}_1, t) \Delta V(\mathbf{r}_2, t) \rangle_{ts} \Psi_0^{(0)}(\mathbf{K}_0, \mathbf{r}_2) \\ &+ (e\gamma)^4 \int d\mathbf{r}_1 \int d\mathbf{r}_2 \int d\mathbf{r}_3 \int d\mathbf{r}_4 \hat{G}(\mathbf{u}_b, \mathbf{r}_1) G(\mathbf{r}_1, \mathbf{r}_2) \\ &\times G(\mathbf{r}_2, \mathbf{r}_3) G(\mathbf{r}_3, \mathbf{r}_4) \langle \Delta V(\mathbf{r}_1, t) \Delta V(\mathbf{r}_2, t) \rangle_{ts} \\ &\times \langle \Delta V(\mathbf{r}_3, t) \Delta V(\mathbf{r}_4, t) \rangle_{ts} \Psi_0^{(0)}(\mathbf{K}_0, \mathbf{r}_4) + \dots \end{aligned} \quad (19a)$$

$$\begin{aligned} \langle \Psi_0(\mathbf{r}, t) \rangle_{ts} &= \Psi_0^{(0)}(\mathbf{K}_0, \mathbf{r}) + (e\gamma)^2 \int d\mathbf{r}_1 \int d\mathbf{r}_2 \\ &\times G(\mathbf{r}, \mathbf{r}_1) G(\mathbf{r}_1, \mathbf{r}_2) \langle \Delta V(\mathbf{r}_1, t) \Delta V(\mathbf{r}_2, t) \rangle_{ts} \Psi_0^{(0)}(\mathbf{K}_0, \mathbf{r}_2) \\ &+ (e\gamma)^4 \int d\mathbf{r}_1 \int d\mathbf{r}_2 \int d\mathbf{r}_3 \int d\mathbf{r}_4 G(\mathbf{r}, \mathbf{r}_1) G(\mathbf{r}_1, \mathbf{r}_2) \\ &\times G(\mathbf{r}_2, \mathbf{r}_3) G(\mathbf{r}_3, \mathbf{r}_4) \langle \Delta V(\mathbf{r}_1, t) \Delta V(\mathbf{r}_2, t) \rangle_{ts} \\ &\times \langle \Delta V(\mathbf{r}_3, t) \Delta V(\mathbf{r}_4, t) \rangle_{ts} \Psi_0^{(0)}(\mathbf{K}_0, \mathbf{r}_4) + \dots \end{aligned} \quad (19b)$$

and  $\Phi_0^{(0)}(\mathbf{K}_0, \mathbf{u}_b, t) = \text{FT}[\Psi_0^{(0)}(\mathbf{K}_0, x, y, \infty)]$ . The even order terms contained in  $\langle \Phi_0(\mathbf{K}_0, \mathbf{u}_b, t) \rangle_{ts}$  denote the absorption effect created by diffuse scattering on the Bragg reflections. This is the conventional absorption effect. The second term of Eq. (18) covers the contributions of the diffusely scattered electrons, which are distributed at non-Bragg positions. It is apparent that all of the high-order terms ( $\Delta V^2, \Delta V^4$ , etc.) have been included. In practice, the numerical calculation is directly performed using Eq. (18) without using the Born series as given in Eqs. (19a) and (19b).

For Fraunhofer diffraction, it can be proved that the two-dimensional Fourier transform of the Green's function is [41]

$$\hat{G}(\mathbf{u}_b, \mathbf{r}_1) = A_z \Psi_0^{(0)}(-\mathbf{K}, \mathbf{r}_1), \quad (20)$$

where  $\Psi_0^{(0)}(-\mathbf{K}, \mathbf{r}_1)$  is the solution of the Schrödinger equation [Eq. (10)] for an incident plane wave of wavevector  $(-\mathbf{K})$  with  $\mathbf{K} = \mathbf{K}_0 + \mathbf{u}_b$  and

$$A_z = \left\{ -\frac{im_0}{\pi\hbar^2} \frac{\exp[2\pi i K_z z]}{K_z} \right\}.$$

The negative sign of the wave vector means that the electron strikes the crystal along the negative  $z$ -axis direction. For a general case,  $\langle \Delta V(\mathbf{r}_1, t) \Delta V^*(\mathbf{r}_2, t) \rangle_{ts}$  is written into a Fourier transform form

$$\begin{aligned} \langle \Delta V(\mathbf{r}_1, t) \Delta V^*(\mathbf{r}_2, t) \rangle_{ts} &= \int d\mathbf{Q} \int d\mathbf{Q}' \\ &\times \exp[2\pi i(\mathbf{r}_1 \cdot \mathbf{Q} - \mathbf{r}_2 \cdot \mathbf{Q}')] S(\mathbf{Q}, \mathbf{Q}'), \end{aligned} \quad (21)$$

where  $S(\mathbf{Q}, \mathbf{Q}')$  is defined as the diffuse scattering dynamic form factor, to be determined for different processes in Section 5. Thus, Eq. (18) is rewritten as

$$\begin{aligned} I(\mathbf{u}_b) &= |\langle \Phi_0(\mathbf{K}_0, \mathbf{u}_b, t) \rangle_{ts}|^2 + D \int d\mathbf{Q} \int d\mathbf{Q}' S(\mathbf{Q}, \mathbf{Q}') \\ &\times \{ \int d\mathbf{r}_1 [\exp(2\pi i(\mathbf{r}_1 \cdot \mathbf{Q})) \\ &\times \Psi_0^{(0)}(-\mathbf{K}_0 - \mathbf{u}_b, \mathbf{r}_1) \Psi_0(\mathbf{K}_0, \mathbf{r}_1)] \\ &\times \int d\mathbf{r}_2 [\exp(-2\pi i\mathbf{r}_2 \cdot \mathbf{Q}') \\ &\times \langle \Psi_0^{(0)*}(-\mathbf{K}_0 - \mathbf{u}_b, \mathbf{r}_2) \rangle_{ts} \langle \Psi_0^*(\mathbf{K}_0, \mathbf{r}_2) \rangle_{ts}] \}, \end{aligned} \quad (22)$$

where  $D = e^2 \gamma^2 m_0 [2\pi^2 \hbar^2 E \cos^2 \varphi_0]^{-1}$ , and  $\varphi_0$  is the angle between  $\mathbf{K}$  and the  $z$ -axis. One must remember that this equation is not restricted by the DWBA, and the multiple scattering terms are included. Eqs. (17) and (22) are the core of the entire calculation. The unique advantage of Eq. (22) is that the time and structure average are performed analytically before numerical calculations. It has been proved that the calculation using Eqs. (6) and (17) preserves the total scattering intensity (see Appendix B). Thus, the approximation made in deriving Eq. (16) does not introduce any appreciable errors at all. The applicability of this theory is not restricted by the magnitude of the surface roughness. For a highly disordered surface, the optical potential  $V$  approaches atomic potential and its real and imaginary components are both important.

## 4. Applications

### 4.1. The Bloch wave theory

The Bethe theory is a classical approach to dynamical electron diffraction, and it is the ideal approach for treating the non-local potential. We start with this theory to illustrate the basic procedures of applying Eqs. (17) and (22) for RHEED calculations. In the Bloch wave representation, the elastic scattering wave of incident wave vector  $\mathbf{K}$  is a linear superposition of Bloch waves  $B_i(\mathbf{K}, \mathbf{r})$  [1]

$$\langle \Psi_0(\mathbf{K}, \mathbf{r}) \rangle = \sum_i \alpha_i(\mathbf{K}) B_i(\mathbf{K}, \mathbf{r}), \quad (23a)$$

where  $\alpha_i(\mathbf{K})$  are the superposition coefficients determined by the boundary conditions,  $B_i(\mathbf{K}, \mathbf{r})$  is the  $i$ th eigen solution of Eq. (17), which is generally given by

$$B_i(\mathbf{K}, \mathbf{r}) = \sum_{\mathbf{g}} C_{\mathbf{g}}^{(i)}(\mathbf{K}) \exp[2\pi i(\mathbf{K} + \mathbf{g}) \cdot \mathbf{r} + 2\pi i v_i x]. \quad (23b)$$

The coefficients  $C_{\mathbf{g}}^{(i)}(\mathbf{K})$  and eigenvalue  $v_i$  are determined by an eigen equation in the Bloch wave theory. Substituting Eqs. (23b) into (17) and using the inverse Fourier transform, a set of coupled algebraic equations are obtained

$$[2KS_{\mathbf{g}} - 2(K_x + g_x)v - v^2]C_{\mathbf{g}}^{(i)} + \frac{2\gamma m_0 e}{\hbar^2} \sum_{\mathbf{h}} [V_{\mathbf{g}-\mathbf{h}} + V'_{\mathbf{g}\mathbf{h}}]C_{\mathbf{h}}^{(i)} = 0, \quad (24)$$

where  $V_{\mathbf{g}}$  are the Fourier coefficients of the crystal potential and those of the complex potential  $V'$  are

$$V'_{\mathbf{g}\mathbf{h}} = \frac{e\gamma}{V_c} \int d\mathbf{Q} \int d\mathbf{Q}' S(\mathbf{Q}, \mathbf{Q}') \times \hat{G}(\mathbf{k}_i + \mathbf{g} - \mathbf{Q}, \mathbf{Q}' - \mathbf{k}_i - \mathbf{h}), \quad (25)$$

$V_c$  is the volume of the crystal, and  $\hat{G}(\mathbf{u}, \mathbf{v})$  is the double Fourier transform of  $G(\mathbf{r}, \mathbf{r}_1)$ . If  $G$  is replaced by  $G_0$ , the Green's function in free-space, after some calculation, Eq. (25) gives [39]

$$V'_{\mathbf{g}\mathbf{h}} \approx \frac{em_0\gamma}{2\pi^2\hbar^2 V_c} \times \left\{ \int d\tau(\mathbf{u}) \frac{S(\mathbf{g} + \mathbf{k}_i - \mathbf{u}, \mathbf{h} + \mathbf{k}_i - \mathbf{u})}{u^2 - K_0^2} + i \frac{\pi}{2K_0} \int d\sigma(\mathbf{u}) S(\mathbf{g} + \mathbf{k}_i - \mathbf{u}, \mathbf{h} + \mathbf{k}_i - \mathbf{u}) \right\}, \quad (26)$$

where the integral  $\tau(\mathbf{u})$  is over all reciprocal space  $\mathbf{u}$  except a spherical shell defined by  $|\mathbf{u}| = K_0$ , and the integral  $\sigma(\mathbf{u})$  is over the Ewald sphere surface defined by  $|\mathbf{u}| = K_0$ . This function is complex, and its real part may not be too small in comparison to the crystal potential, particularly for a rough surface in RHEED. The imaginary component is just the absorption potential that has been fre-

quently used in dynamical calculations. Eq. (26) is the familiar form of absorption potential in high-energy electron diffraction [39]. However, this potential is not suitable for recovering the high-order scattering terms, a calculation of  $V'_{\mathbf{g}\mathbf{h}}^{(i)}$  with consideration of dynamic diffraction is necessary (Appendix C).

For the diffuse scattering intensity, substituting Eqs. (23a) and (23b) into the second term of Eq. (22), and performing the integrals, the diffuse scattering intensity at  $\mathbf{u}_b$  in reciprocal space is

$$I_D(\mathbf{u}_b) = D \sum_i \sum_j \sum_{i'} \sum_{j'} \sum_{\mathbf{g}} \sum_{\mathbf{h}} \sum_{\mathbf{g}'} \sum_{\mathbf{h}'} \times \alpha_{i'}(-\mathbf{K}) \alpha_j^*(-\mathbf{K}) \alpha_{i'}(\mathbf{K}_0) \alpha_j^*(\mathbf{K}_0) \times C_{\mathbf{g}}^{(i)}(-\mathbf{K}) C_{\mathbf{h}}^{(j)*}(-\mathbf{K}) C_{\mathbf{g}'}^{(i')}(\mathbf{K}_0) C_{\mathbf{h}'}^{(j')}(\mathbf{K}_0) \times \int dQ_x \int dQ_x' S(\mathbf{Q}, \mathbf{Q}') \times \int_0^{\infty} dx_1 \exp[2\pi i(Q_x + g_x + g_x' + v_i + v_{i'})x_1] \times \int_0^{\infty} dx_2 \exp[-2\pi i(Q_x' + h_x + h_x' + v_j + v_{j'})x_2], \quad (27a)$$

where

$$\mathbf{Q}_t = \mathbf{u}_t - \mathbf{g}_t - \mathbf{g}_t', \quad (27b)$$

$$\mathbf{Q}_t' = \mathbf{u}_t - \mathbf{h}_t - \mathbf{h}_t', \quad (27c)$$

$\mathbf{K} = \mathbf{K}_0 + \mathbf{u}_b$ ,  $\mathbf{g}$  and  $\mathbf{h}$  are reciprocal lattice vectors, and the subscript t means the tangential component parallel to the (y,z) surface plane.  $\{\alpha_i, C_{\mathbf{g}}^{(i)}\}$  and  $\{\alpha_i', C_{\mathbf{g}}^{(i)'}\}$  are the solution of Eq. (24) with and without the inclusion of  $V'_{\mathbf{g}\mathbf{h}}^{(i)}$ , respectively. The sums of  $i, j, i'$  and  $j'$  are over all the Bloch waves, and the sums of  $\mathbf{g}, \mathbf{h}, \mathbf{g}'$  and  $\mathbf{h}'$  are over all the reciprocal lattice vectors. In Eq. (27a), the  $\alpha$ s and  $C$ s coefficients characterize the dynamical diffraction before and after diffuse scattering. Eqs. (27b) and (27c) are the results of momentum conservation parallel to the surface.

#### 4.2. The parallel-to-surface multi-slice theories

If the non-periodic modulation of the potential occurs only in the direction normal to the surface, the parallel-to-surface multi-slice theories [7–14] are most useful for quantitative RHEED calcula-

tions. In this model, the crystal potential is written as

$$V_0(\mathbf{r}) = \sum_{\mathbf{g}} V_{\mathbf{g}}(x) \exp[2\pi i \mathbf{g} \cdot \boldsymbol{\rho}], \quad (28)$$

where  $\boldsymbol{\rho} = (y, z)$  is a real-space vector parallel to the surface, and the Fourier coefficients  $V_{\mathbf{g}}(x)$  are  $x$ -dependent, which can be modified to include surface relaxation and surface potential. The solution of Eq. (17) can be written as

$$\langle \Psi_0(\mathbf{K}, \mathbf{r}) \rangle = \sum_{\mathbf{g}} \Psi_{\mathbf{g}}(\mathbf{K}, x) \exp[2\pi i (\mathbf{K}_t + \mathbf{g}_t) \cdot \boldsymbol{\rho}], \quad (29)$$

where  $\mathbf{K}_t$  and  $\mathbf{g}_t$  are the tangential components of  $\mathbf{K}$  and  $\mathbf{g}$ , respectively, parallel to the surface. To simplify the calculation, the complex potential is approximated as a local function so that  $\Psi_0$  can be taken out of the integral, Eq. (17) becomes

$$\left( -\frac{\hbar^2}{2m_0} \nabla^2 - e\gamma V_0 - E \right) \Psi_0 \approx (e\gamma^2 [\int d\mathbf{r}_1 [G(\mathbf{r}, \mathbf{r}_1) \langle \Delta V(\mathbf{r}, t) \times \Delta V(\mathbf{r}_1, t) \rangle_{\text{is}}] \langle \Psi_0(\mathbf{K}_0, \mathbf{r}) \rangle). \quad (30)$$

This approximation holds for most of the cases in RHEED [42]. Substituting Eqs. (29) into (30), a double differential equation is obtained

$$\frac{d^2 \Psi_{\mathbf{g}}(\mathbf{K}, x)}{dx^2} + \Gamma_{\mathbf{g}}^2 \Psi_{\mathbf{g}}(\mathbf{K}, x) + \frac{2\gamma m_0 e}{\hbar^2} \sum_{\mathbf{h}} [V_{\mathbf{g}-\mathbf{h}}(x) + V'_{\mathbf{g}\mathbf{h}}(x)] \Psi_{\mathbf{h}}(\mathbf{K}, x) = 0, \quad (31a)$$

where

$$\Gamma_{\mathbf{g}}^2 = 4\pi^2 [K^2 - (\mathbf{K}_t + \mathbf{g}_t)^2], \quad (31b)$$

$$V'_{\mathbf{g}\mathbf{h}}(x) = \frac{e\gamma}{S_c} \int d\mathbf{Q} \int d\mathbf{Q}' S(\mathbf{Q}, \mathbf{Q}') \times \int d\boldsymbol{\rho} \int d\mathbf{r}_1 \exp[-2\pi i \boldsymbol{\rho} \cdot (\mathbf{K}_t + \mathbf{g}_t - \mathbf{Q})] \times \exp[-2\pi i \mathbf{r}_1 \cdot (\mathbf{Q}' - \mathbf{K}_t - \mathbf{h}_t)] G(x, \boldsymbol{\rho}, \mathbf{r}_1). \quad (31c)$$

$S_c$  is the area of the crystal surface stroke by the beam. The calculation of  $V'_{\mathbf{g}\mathbf{h}}$  for a general case is given in Appendix C). Eq. (31a) is a coupled second-order differential equation, the solutions of which are the amplitudes of the diffracted beams.

Eq. (31a) can be solved numerically using various techniques [7–14], all of which are based on the same physical approach of cutting the crystal into slices parallel to the surface, but they are slightly different in mathematical treatments. The key step in each of these approaches is to transform the second-order differential equation into a first-order differential equation.

Our task here is to calculate the diffuse scattering pattern. Substituting Eq. (29) into the second term of Eq. (22), and performing the integrals, one has

$$I_D(\mathbf{u}_b) = D \sum_{\mathbf{g}} \sum_{\mathbf{h}} \sum_{\mathbf{g}'} \sum_{\mathbf{h}'} \int_0^{\infty} dx_1 \int_0^{\infty} dx_2 \times \Psi_{\mathbf{g}}^{(0)}(-\mathbf{K}, x_1) \Psi_{\mathbf{h}}^{(0)*}(-\mathbf{K}, x_2) \Psi_{\mathbf{g}'}(\mathbf{K}_0, x_1) \times \Psi_{\mathbf{h}'}^*(\mathbf{K}_0, x_2) \times \int dQ_x \int dQ'_x S(\mathbf{Q}, \mathbf{Q}') \times \exp[2\pi i (Q_x x_1 - Q'_x x_2)], \quad (32a)$$

where

$$Q_z = -g_z - g'_z \text{ and } Q_y = u_y - g_y - g'_y, \quad (32b)$$

$$Q_{z'} = -h_z - h'_z \text{ and } Q_{y'} = u_y - h_y - h'_y, \quad (32c)$$

and  $\mathbf{K} = \mathbf{K}_0 + \mathbf{u}_b$ . In Eq. (32a),  $\{\Psi_{\mathbf{g}}\}$  and  $\Psi_{\mathbf{g}}^0$  are the solutions of Eq. (31a) with and without the inclusion of  $V'_{\mathbf{g}\mathbf{h}}$ , respectively. Eq. (32b) and Eq. (32c) are the results of momentum conservation parallel to the surface.

### 4.3. The perpendicular-to-surface multi-slice theory

In this multi-slice theory, the slices are cut perpendicular to the surface, and the theory offers a unique advantage for automatically including surface point vacancies and short-range ordering because the atomic arrangement in each slice can be chosen differently [15]. However, the unit cell truncated in the calculation is so large as to ensure the statistical average over different lattice configurations. Recently, this theory has been applied to calculate the RHEED patterns of the  $\text{Cu}_3\text{Au}(111)$  surface, which shows short-range order due to the site substitution of Cu by Au [43], and a remarkable success has been demonstrated.

## 5. Calculation of the dynamic form factor $S(\mathbf{Q}, \mathbf{Q}')$

Based on the theory presented in Section 4, diffuse scattering due to both TDS and point vacancies can be calculated using the available theoretical approaches, provided the dynamic form factor  $S(\mathbf{Q}, \mathbf{Q}')$  is known. The calculation of this factor is the task for this section.

### 5.1. Thermal diffuse scattering

We first concentrate on the calculation of the dynamic form factor  $S$  for TDS. In a crystal, each atom is vibrating around its average equilibrium position. The instantaneous position of the  $\kappa$ th atom in the crystal is  $\mathbf{r}_{\kappa'} = \mathbf{r}_{\kappa} + \mathbf{U}_{\kappa}(t)$ , where  $\mathbf{U}_{\kappa}$  is the instantaneous displacement of the atom from its equilibrium position  $\mathbf{r}_{\kappa}$ , and depends on time and the position of the atom, particularly in the case of surface atoms in RHEED. In TDS, we first do not consider the point vacancies introduced in crystal lattices, and thus the average of  $\langle \Delta V(\mathbf{r}_1, t) \Delta V(\mathbf{r}_2, t) \rangle_t$  is on time only. This calculation can be conveniently performed if the crystal potential is expressed as a Fourier transform of the scattering factors [28]

$$\begin{aligned} \Delta V(\mathbf{r}_1, t) &= V(\mathbf{r}_1, t) - V_0(\mathbf{r}_1, t) \\ &= \sum_{\kappa} \int d\boldsymbol{\tau} \exp[2\pi i(\mathbf{r}_1 - \mathbf{r}_{\kappa}) \cdot \boldsymbol{\tau}] f_{\kappa}^e(\boldsymbol{\tau}) \\ &\quad \times \{ \exp(-2\pi i \mathbf{U}_{\kappa} \cdot \boldsymbol{\tau}) - \exp[-W_{\kappa}(\boldsymbol{\tau})] \}, \end{aligned} \quad (33)$$

where  $\boldsymbol{\tau}$  is a reciprocal space vector,  $f_{\kappa}^e(\boldsymbol{\tau})$  is the electron scattering factor of the  $\kappa$ th atom, and  $W_{\kappa}(\boldsymbol{\tau}) = 2\pi^2 \langle |\boldsymbol{\tau} \cdot \mathbf{U}_{\kappa}|^2 \rangle_t$  is the Debye–Waller factor. The sum of  $\kappa$  is over all the atoms in the crystal and on the surface. Thus

$$\begin{aligned} \langle \Delta V(\mathbf{r}_1, t) \Delta V^*(\mathbf{r}_2, t) \rangle_t &= \sum_{\kappa} \sum_{\kappa'} \int d\boldsymbol{\tau} \int d\mathbf{u} \\ &\quad \times \exp[2\pi i(\mathbf{r}_1 - \mathbf{r}_{\kappa}) \cdot \boldsymbol{\tau}] \\ &\quad \times \exp[-2\pi i(\mathbf{r}_2 - \mathbf{r}_{\kappa'}) \cdot \mathbf{u}] f_{\kappa}^e(\boldsymbol{\tau}) [f_{\kappa'}^e(\mathbf{u})]^* \\ &\quad \times \langle \{ \exp(-2\pi i \mathbf{U}_{\kappa} \cdot \boldsymbol{\tau}) - \exp[-W_{\kappa}(\boldsymbol{\tau})] \} \\ &\quad \times \{ \exp(2\pi i \mathbf{U}_{\kappa'} \cdot \mathbf{u}) - \exp[-W_{\kappa'}(\mathbf{u})] \} \rangle_t. \end{aligned} \quad (34)$$

Comparing Eqs. (34) with (21), the dynamic form factor for TDS is

$$\begin{aligned} S(\mathbf{Q}, \mathbf{Q}') &= \sum_{\kappa} \sum_{\kappa'} [f_{\kappa}^e(\mathbf{Q}) [f_{\kappa'}^e(\mathbf{Q}')]^* \\ &\quad \times \exp[-2\pi i \mathbf{Q} \cdot \mathbf{r}_{\kappa} + 2\pi i \mathbf{Q}' \cdot \mathbf{r}_{\kappa'}] \\ &\quad \times \exp[-W_{\kappa}(\mathbf{Q}) - W_{\kappa'}(\mathbf{Q}')] \\ &\quad \times \{ \exp[2F_{\kappa\kappa'}(\mathbf{Q}, \mathbf{Q}')] - 1 \}, \end{aligned} \quad (35a)$$

where a correlation function is defined

$$F_{\kappa\kappa'}(\mathbf{Q}, \mathbf{Q}') = 4\pi^2 \langle (\mathbf{Q} \cdot \mathbf{U}_{\kappa})(\mathbf{Q}' \cdot \mathbf{U}_{\kappa'}) \rangle_t, \quad (35b)$$

which describes the correlation between atom vibrations.

For the calculation here, the vibration of surface atoms is assumed to be described by the same lattice dynamics as for the atoms in a large bulk crystal. Based on the harmonic oscillators and adiabatic approximations, in which all the atoms are assumed to interact with harmonic forces and the crystal electrons move as though the ions were fixed in their instantaneous positions, one considers the phonon modes existing in a perfect crystal of infinite number of unit cells. The summation over  $\kappa$  can be separated into a summation over centers of unit cells  $\mathbf{R}_n$  and a summation over atoms within a cell, the equilibrium position of the  $\alpha$ th atom relative to the  $n$ th unit cell is  $\mathbf{r}_{\kappa} = \mathbf{R}_n + \mathbf{r}(\alpha)$ , and time-dependent displacement vector of the  $\kappa$ th atom is given in normal coordinates as [44]

$$\begin{aligned} \mathbf{U}_{\kappa} &= \frac{\hbar^{1/2}}{(2N_0 M_{\kappa})^{1/2}} \sum_{\mathbf{q}} \sum_j \frac{1}{\omega_j(\mathbf{q})^{1/2}} \\ &\quad \times e(\kappa|\mathbf{q}) \exp[2\pi i \mathbf{q} \cdot \mathbf{r}_{\kappa}] [a^+(\mathbf{q}) + a(\mathbf{q})], \end{aligned} \quad (36)$$

where  $\mathbf{q}$ ,  $\omega_j(\mathbf{q})$  and  $e$  are the phonon momentum, frequency and polarization vectors, respectively,  $N_0$  is the total number of primitive unit cells in the crystal,  $M_{\kappa}$  is the mass of the  $\kappa$ th atom,  $j$  indicates phonon branches, and  $a^+(\mathbf{q}_j)$  and  $a(\mathbf{q}_j)$  are defined as the creation and annihilation operators of a phonon with wave vector  $\mathbf{q}$  and frequency  $\omega_j$ .

In RHEED, anisotropic vibration of surface atoms might be important because of the broken bonding at the surface. It has been shown that the contribution made by surface phonons is compara-

ble to that made by the phonons in the bulk [45]. To introduce this effect in the calculation, the phonon dispersion  $\omega_j(\mathbf{q})$  and the polarization vector  $\mathbf{e}(\alpha|\mathbf{q}_j)$  are modified in such a way that they are assumed to depend not only on the position of the atom (at the surface or in the bulk) but also on the vibration direction; thus  $\omega_j(\mathbf{q})$  is replaced by  $\omega_j(s_\kappa, \mathbf{q})$ , where  $\omega_j(s_\kappa, \mathbf{q}) = \omega_j(\mathbf{q})$  if the atom is in the bulk and it can be different if the atom is at the surface,  $\mathbf{e}(\alpha|\mathbf{q}_j)$  is separated into components parallel ( $e_i$ ) and perpendicular ( $e_x$ ) to the surface

$$\mathbf{e}(\alpha|\mathbf{q}_j) = e_i(\kappa|\mathbf{q}_j) + e_x(\kappa|\mathbf{q}_j)\hat{x}. \quad (37)$$

In the high-temperature limiting case

$$\begin{aligned} F_{\kappa\kappa'}(\mathbf{Q}, \mathbf{Q}') &\approx 2\pi^2 \Omega \\ &\times \int_{\text{BZ}} d\mathbf{q} \sum_j \frac{k_B T}{\omega_j(s_\kappa, \mathbf{q}) \omega_j(s_{\kappa'}, \mathbf{q}) (M_\kappa M_{\kappa'})^{1/2}} \\ &\times [\mathbf{Q} \cdot \mathbf{e}(\kappa|\mathbf{q})][\mathbf{Q}' \cdot \mathbf{e}(\kappa'|\mathbf{q}')] \\ &\times \exp[2\pi i \mathbf{q} \cdot (\mathbf{r}_\kappa - \mathbf{r}_{\kappa'})], \end{aligned} \quad (38)$$

where  $\Omega$  is the volume of the unit cell, and the integration of  $\mathbf{q}$  is restricted to the first Brillouin zone (BZ). The orientation average of  $[\mathbf{Q} \cdot \mathbf{e}][\mathbf{Q}' \cdot \mathbf{e}]$  is evaluated by assuming that the vibration displacements in the  $y$ - $z$  plane (parallel to the surface) and in the  $x$ -axis direction (perpendicular to the surface) are different, one has approximately

$$[\mathbf{Q} \cdot \mathbf{e}(\kappa|\mathbf{q})][\mathbf{Q}' \cdot \mathbf{e}(\kappa'|\mathbf{q}')] \approx \frac{Q_x Q'_x \beta_s + Q_y Q'_y + Q_z Q'_z}{3} \quad (39)$$

where  $\beta_s$  is the ratio between the mean square atom vibration amplitudes perpendicular to and parallel to the surface.  $\beta_s = 1$  if the atom is located in the bulk. Thus

$$\begin{aligned} F_{\kappa\kappa'}(\mathbf{Q}, \mathbf{Q}') &\approx \frac{Q_x Q'_x \beta_s + Q_y Q'_y + Q_z Q'_z}{3} \Omega \\ &\times \int_{\text{BZ}} d\mathbf{q} \sum_j \frac{2\pi^2 k_B T}{\omega_j(s_\kappa, \mathbf{q}) \omega_j(s_{\kappa'}, \mathbf{q}) (M_\kappa M_{\kappa'})^{1/2}} \\ &\times \exp[2\pi i \mathbf{q} \cdot (\mathbf{r}_\kappa - \mathbf{r}_{\kappa'})]. \end{aligned} \quad (40)$$

To simplify Eq. (40), the Warren approximation is introduced [46]. We assume that all vibration waves can be considered as either purely longitudinal or purely transverse. The velocities of all longi-

tudinal waves are replaced by an average longitudinal velocity, and the velocities of all transverse waves by an average transverse velocity. Each average velocity is considered to be a constant independent of the phonon-wave vector  $\mathbf{q}$ . To perform the integral over  $\mathbf{q}$  in Eq. (37), the Brillouin zone is replaced by a sphere of radius  $q_m$ , whose volume is equal to that of the Brillouin zone  $\frac{4}{3} \pi q_m^3 = V_{\text{BZ}} = 1/\Omega$ . For a cubic crystal with lattice constant  $a$ ,  $q_m = 3^{1/3} (4\pi)^{-1/3} a^{-1}$ . The density of points (or states) in the sphere is  $N_0/V_{\text{BZ}}$ , and the summation of  $\mathbf{q}$  is replaced by an integration throughout the sphere. For each type of wave, longitudinal or transverse, the polarization vector  $\mathbf{e}$  takes with equal probability at all orientations relative to  $\boldsymbol{\tau}$ , and for all waves whose vector  $\mathbf{q}$  terminate in the hollow sphere, we can use the average  $\langle [\mathbf{Q} \cdot \mathbf{e}][\mathbf{Q}' \cdot \mathbf{e}] \rangle = \mathbf{Q} \cdot \mathbf{Q}'/3$ . Defining  $\omega_{jm} = 2\pi v_j q_m$  for the acoustic branches, which are assumed to be dominant modes for atom displacements, where  $v_j$  is the velocity of the phonon, one has

$$\begin{aligned} F_{\kappa\kappa'}(\mathbf{Q}, \mathbf{Q}') &\approx \frac{3k_B T (Q_x Q'_x \beta_s + Q_y Q'_y + Q_z Q'_z)}{2q_m^2 (M_\kappa M_{\kappa'})^{1/2}} \\ &\times \left[ \sum_j \frac{1}{v_{jk} v_{jk'}} \right] \frac{\text{Si}(\Theta_{\kappa\kappa'})}{\Theta_{\kappa\kappa'}} \\ &= 2\pi^2 a^2 \frac{M_\kappa^{1/2}}{M_{\kappa'}^{1/2}} (Q_x Q'_x \beta_s \\ &+ Q_y Q'_y + Q_z Q'_z) \\ &\times \frac{\sum_j (v_{jk} v_{jk'})^{-1} \text{Si}(\Theta_{\kappa\kappa'})}{\sum_j v_{jk}^{-2} \Theta_{\kappa\kappa'}}, \end{aligned} \quad (41)$$

where the phonon velocity  $v_{jk} = v_j$  if the atom is in the bulk, it might be different otherwise

$$\text{Si}(\Theta) = \int_0^\Theta du \frac{\sin u}{u}, \quad (42)$$

with  $\Theta_{\kappa\kappa'} = 2\pi q_m |\mathbf{r}_\kappa - \mathbf{r}_{\kappa'}|$ .  $\text{Si}(\Theta)$  is a function which describes the vibration correlation between atoms and characterizes the coherent property of the diffuse scattering waves generated within a local region [47].  $\text{Si}(\Theta_{\kappa\kappa'})/\Theta_{\kappa\kappa'}$  drops quickly with

increasing interatomic distance (see Fig. 4). By assuming a 10% cut-off,  $2\pi q_m |r_k - r_{k'}|_{\max} \approx 10$ . For  $a = 0.4$  nm, the coherent length is  $|r_k - r_{k'}|_{\max} \approx 1$  nm, about 4–5 interatomic distances. If two atoms are separated by more than 1 nm, the TDS waves generated from the two atom sites are incoherent. This is the result from the Debye model rather than the Einstein model assumed in some of the published papers.

### 5.2. Diffuse scattering produced by a growing surface

A growing surface can be considered to have a surface coverage  $\chi_0$ . In the top growing layer, some

of the lattices are filled with atoms and the remaining ones are vacant. The sites filled with atoms can be aggregated to form surface islands, surface steps or random points, depending on the growth temperature. The following treatment is designed for a general case, and the distribution of point vacancies varies from cell to cell. Therefore, a structural average on different cell configurations must be made to statistically average over the randomness and ordering of point vacancies produced by surface roughness. For simplicity, we consider a case in which the crystal structure is dominated by a periodic lattice, but with some point vacancies. The point vacancies can be attributed to the sites that have not been filled by atoms at the surface,

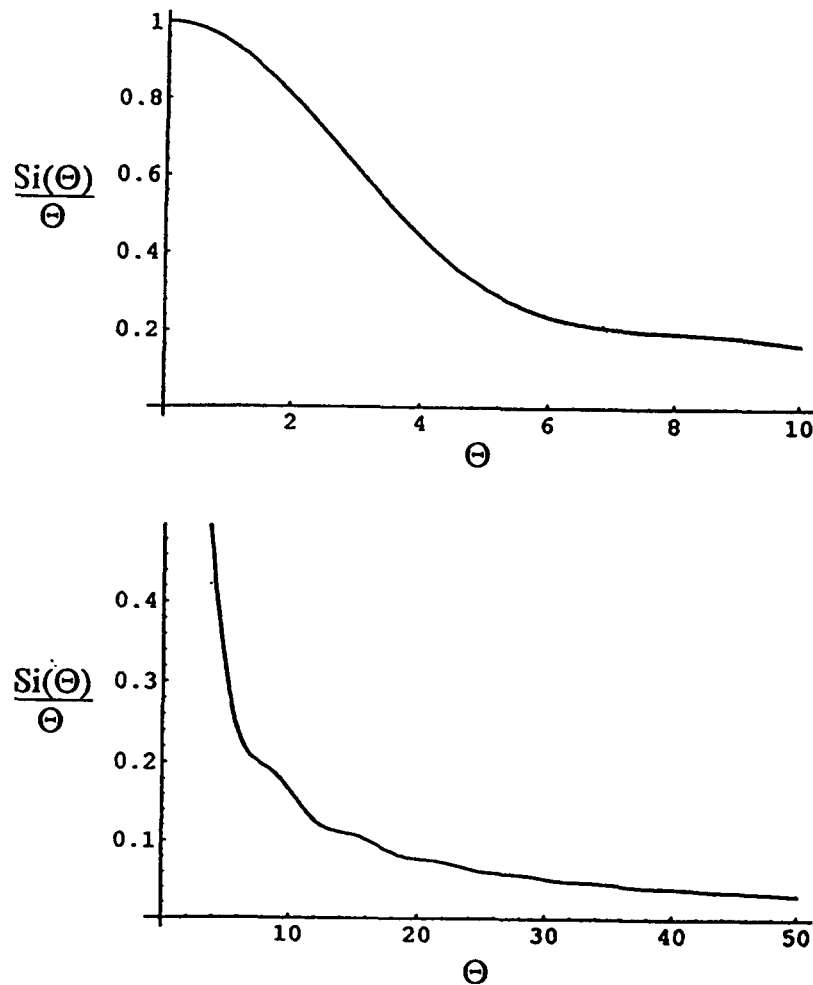


Fig. 4. Plots of the function  $Si(\Theta)/\Theta$ .

as schematically shown in figure 8. This is a typical case in MBE growth. Thus, the crystal potential is written as

$$V(\mathbf{r}, t) = \sum_{\kappa} \int d\boldsymbol{\tau} \exp[2\pi i(\mathbf{r} - \mathbf{r}_{\kappa} - \mathbf{U}_{\kappa}) \cdot \boldsymbol{\tau}] \sigma_{\kappa}(x) f_{\kappa}^e(\boldsymbol{\tau}), \quad (43)$$

with  $\sigma_{\kappa}(x) = 1$  if the site is occupied and  $\sigma_{\kappa}(x) = 0$  if the site is vacant [37]. The operator  $\sigma_{\kappa}(x)$  is  $x$  dependent in order to take into account the dependence of vacancy distribution as a function of depth into the surface. The structure average is to effectively reduce the scattering power of each atom, and then

$$V_0(\mathbf{r}) = \chi_0(x) \sum_{\kappa} \int d\boldsymbol{\tau} \times \exp[2\pi i(\mathbf{r} - \mathbf{r}_{\kappa}) \cdot \boldsymbol{\tau}] f_{\kappa}^e(\boldsymbol{\tau}) \exp[-W_{\kappa}(\boldsymbol{\tau})], \quad (44)$$

$\chi_0(x) = \langle \sigma_{\kappa}(x) \rangle_s = 1 - \chi_v(x)$ , where  $\chi_v(x)$  is a depth-dependent probability function of a site to be vacant.  $\chi_0(x)$  can be understood as the depth-dependent coverage of each growing layer in MBE. TDS always accompanies electron scattering and it cannot be separated from the diffuse scattering caused by point vacancies. Thus, for a non-perfect crystal TDS must also be considered. Hence

$$\begin{aligned} & \langle \Delta V(\mathbf{r}_1, t) \Delta V^*(\mathbf{r}_2, t) \rangle_{ts} \\ &= \sum_{\kappa} \sum_{\kappa'} \int d\boldsymbol{\tau} \int d\mathbf{u} \\ & \times \exp[2\pi i(\mathbf{r}_1 - \mathbf{r}_{\kappa}) \cdot \boldsymbol{\tau}] \\ & \times \exp[-2\pi i(\mathbf{r}_2 - \mathbf{r}_{\kappa'}) \cdot \mathbf{u}] f_{\kappa}^e(\boldsymbol{\tau}) [f_{\kappa'}^e(\mathbf{u})]^* \\ & \times \exp[-W_{\kappa}(\boldsymbol{\tau}) - W_{\kappa'}(\mathbf{u})] \{ \langle \sigma_{\kappa}(x_1) \sigma_{\kappa'}(x_2) \rangle_s \\ & \exp[4\pi^2 \langle (\mathbf{U}_{\kappa} \cdot \boldsymbol{\tau})(\mathbf{U}_{\kappa'} \cdot \mathbf{u}) \rangle_t] - \chi_0(x_1) \chi_0(x_2) \}. \end{aligned} \quad (45)$$

The statistical structure average of  $\langle \sigma_{\kappa}(x_1) \sigma_{\kappa'}(x_2) \rangle_s$  is performed as follows. Using the Flinn sign [48]

$$\delta\sigma_{\kappa} = \sigma_{\kappa} - \chi_0 = \chi_v - \sigma_{\kappa}^v, \quad (46)$$

where  $\sigma_{\kappa}^v$  is a vacancy operator with  $\sigma_{\kappa}^v = 0$  if the site is occupied, and  $\sigma_{\kappa}^v = 1$  if the site is vacant.

$$\begin{aligned} \langle \sigma_{\kappa}(x_1) \sigma_{\kappa'}(x_2) \rangle_s &= \langle [\delta\sigma_{\kappa}(x_1) \delta\sigma_{\kappa'}(x_2)] \rangle_s \\ &+ \chi_0(x_1) \chi_0(x_2). \end{aligned} \quad (47)$$

This quantity is correlated to Cowley's SRO

parameter defined by [50]

$$\alpha_{\kappa\kappa'} = \frac{\langle \delta\sigma_{\kappa} \delta\sigma_{\kappa'} \rangle_s}{\chi_0 \chi_v}, \quad (48)$$

with  $\alpha_{\kappa\kappa} = 1$ . Substituting Eqs. (47) and (48) into (45), and comparing with Eq. (21), the dynamic form factor is

$$\begin{aligned} S(\mathbf{Q}, \mathbf{Q}') &= \sum_{\kappa} \sum_{\kappa'} \exp[2\pi i(\mathbf{r}_{\kappa'} \cdot \mathbf{Q} - \mathbf{r}_{\kappa} \cdot \mathbf{Q}')] \\ & \times f_{\kappa}^e(\mathbf{Q}) [f_{\kappa'}^e(\mathbf{Q}')]^* \exp[-W_{\kappa}(\mathbf{Q}) - W_{\kappa'}(\mathbf{Q}')] \\ & \times \left\{ \chi_0 \chi_v \alpha_{\kappa\kappa'} \exp[2F_{\kappa\kappa'}(\mathbf{Q}, \mathbf{Q}')] \right. \\ & \left. + \chi_0(x_1) \chi_0(x_2) \{ \exp[2F_{\kappa\kappa'}(\mathbf{Q}, \mathbf{Q}')] - 1 \} \right\}. \end{aligned} \quad (49)$$

In { }, the first term is the diffuse scattering due to point vacancies, and the second term is due to TDS. If the atomic vibration is described by the Einstein model and there is no correlation in the distribution of the point defects, Eq. (49) gives the result of Dudarev et al. [49]

To show the physical meaning of the SRO parameters, we now examine the relationship between  $\langle \delta\sigma_{\kappa} \delta\sigma_{\kappa'} \rangle$  and the correlation probability. From Eq. (46), the probability of finding an vacancy at a given distance  $\mathbf{r}_{\kappa\kappa'}$  from a vacancy at site  $\kappa$  is

$$\begin{aligned} P_{\kappa\kappa'}^{vv} &= \langle \sigma_{\kappa}^v \sigma_{\kappa'}^v \rangle \\ &= \langle (\chi_v - \delta\sigma_{\kappa})(\chi_v - \delta\sigma_{\kappa'}) \rangle_s \\ &= \chi_v^2 + \langle \delta\sigma_{\kappa} \delta\sigma_{\kappa'} \rangle_s = \chi_v^2 + \chi_0 \chi_v \alpha_{\kappa\kappa'}, \end{aligned} \quad (50)$$

where the first term  $\chi_v^2$  represents the probability of two vacancies being distributed at  $\kappa$  and  $\kappa'$  if there is no correlation (i.e. random distribution). Each vacancy site is a point defect. The values of  $\langle \delta\sigma_{\kappa} \delta\sigma_{\kappa'} \rangle_s$  specify the degree to which the neighbors of one vacancy tend to be preferably of the same type of vacancy. If  $\alpha_{\kappa\kappa'}$  is positive,  $P_{\kappa\kappa'}^{vv} > \chi_v^2$ , the vacancies tend to clump together with vacancies. If  $\alpha_{\kappa\kappa'}$  is negative,  $P_{\kappa\kappa'}^{vv} < \chi_v^2$ , the vacancies tend to clump together with atoms. Therefore, the measurement of  $\alpha_{\kappa\kappa'}$  can reflect the short-range ordering in the considered system. The

decrease of  $\alpha_{\kappa\kappa'}$  with the increase of  $r_{\kappa\kappa'}$  gives the range of ordering.

Point vacancies can cause lattice relaxation in the crystal. If there is no correlation between vacancies, the relaxation effect can be taken into account by introducing a similar quantity to the Debye–Waller factor that depends on the average displacement of an atom as a result of lattice relaxation [51]. Although lattice relaxation was not considered in the above derivation, it can easily be included in the calculation by substituting the Debye–Waller factor  $W_{\kappa}(\mathbf{Q})$  by  $[W_{\kappa}(\mathbf{Q}) + W_{\kappa}^{(d)}(\mathbf{Q})]$ , where  $W_{\kappa}^{(d)}(\mathbf{Q}) = 2\pi^2 Q^2 \langle v^2 \rangle$ , and  $\langle v^2 \rangle$  is the mean square displacement produced by lattice relaxation.

In RHEED, formation of island on the surface is an important phenomenon in MBE growth. The calculation of the dynamic form factor for this case has been considered by Beeby [31]. The theory given in this section has also been applied to calculate the dynamic form factor in a binary alloy system, such as  $\text{Cu}_3\text{Au}$ , due to site substitution. Details are reported separately [52,53].

Finally, it is necessary to point out the differences between this theory and the theory presented by Dudarev et al. [42,49]. The contribution of diffuse scattering on the dynamical diffraction intensities is two-fold: how random fluctuations in the atomic arrangement influence the wave function describing elastic Bragg scattering, and what the angular distribution of diffusely scattered electron is. The calculation in Ref. [42] is concentrated on the first question, while the current theory is concentrated on both questions. The current theory has three advantages in comparison to that in Ref. [49]. First, in this theory, the multiple diffuse scattering terms are automatically included, although the calculation is performed using the first-order diffuse scattering equation. In ref. [49], however, it is necessary to solve the integral density matrix equation (Eq. (15) in Ref. [49]) iteratively in order to include the high-order diffuse scattering terms. This can be a process involving a lot of computations. Second, although the theory in Ref. [49] was presented in a general form, the numerical calculation was performed based on the DWBA (Eq. (40) in Ref. [49]). Thus, the result is accurate if the surface distortion is small. In contrast, the theory here is a general approach which is expected

to be applicable to any rough surfaces. It is known that DWBA is a poor approximation for dealing with point defects, because the distorted potential has almost the magnitude of the atomic potential (see Fig. 1) although the surface coverage could be small. Finally, the dynamic form factor is calculated using the Debye model with consideration of the spatial correlation between vacancy distribution, while the calculation in Ref. [49] is based on the Einstein model and random distribution of surface atoms. The atom distribution due to the formation of surface island or steps, in principle, can be properly included in the theory here.

## 6. Conclusions

In this paper, a formal dynamical theory of RHEED has been developed to calculate the diffuse scattering produced by both atom vibrations and point vacancies at surfaces. The theory is aimed at recovering the multiple diffuse scattering that has been dropped by the distorted-wave Born approximation (DWBA). With inclusion of a complex potential in the dynamical calculation, a rigorous proof is given to show that the high-order diffuse scattering terms are recovered in the calculation using the equation originally derived under the DWBA. This conclusion establishes the basis for expanding the RHEED theories developed under the first-order diffuse scattering to cases where the degree of surface roughness is high, allowing dynamical calculations of RHEED rocking curves for any growing surfaces. The time and structure averages over the distorted crystal potential are performed analytically before the numerical calculation. The theory is given in the Bloch wave and multi-slice forms best suited to numerical calculations. The dynamic form factor is calculated with consideration of anisotropic surface-atom vibration and point vacancies at a growing surface. The coherent effect in thermal diffuse scattering introduced by the phase correlation among atom vibrations has been included. It is believed that this general theory will have a profound impact on the implications of existing RHEED theories.

## Appendix A

We now derive the form of  $V$ , which using Eq. (6) would be the exact solution of Eq. (2). By rewriting Eq. (7) into the form

$$\left(-\frac{\hbar^2}{2m_0}\nabla^2 - e\gamma V_0 - E\right)\Psi_0 = e\gamma[V'\Psi_0], \quad (\text{A1})$$

substituting Eqs. (6) into (2) and using Eq. (4)

$$\begin{aligned} & \left(-\frac{\hbar^2}{2m_0}\nabla^2 - e\gamma V_0 - e\gamma\Delta V - E\right)\Psi \\ &= \left(-\frac{\hbar^2}{2m_0}\nabla^2 - e\gamma V_0 - E\right)\Psi - e\gamma\Delta V\Psi \\ &= e\gamma[V'\Psi_0] + e\gamma\Delta V\Psi_0 - e\gamma\Delta V\{\Psi_0(\mathbf{K}_0, \mathbf{r}) \\ &+ \int d\mathbf{r}_1 G(\mathbf{r}, \mathbf{r}_1)[e\gamma\Delta V(\mathbf{r}_1, t)\Psi_0(\mathbf{r}_1, t)]\} \\ &= e\gamma[V'\Psi_0] - e\gamma\Delta V \int d\mathbf{r}_1 G(\mathbf{r}, \mathbf{r}_1)[e\gamma\Delta V(\mathbf{r}_1, t)\Psi_0(\mathbf{r}_1, t)] \\ &= 0. \end{aligned} \quad (\text{A2})$$

thus

$$[V'\Psi_0] = \int d\mathbf{r}_1 G(\mathbf{r}, \mathbf{r}_1)[e\gamma\Delta V(\mathbf{r}, t)\Delta V(\mathbf{r}_1, t)]\Psi_0(\mathbf{r}_1, t). \quad (\text{A3})$$

This is just Eq. (8).

## Appendix B

From Eqs. (17) and (22), the diffraction intensity is calculated based on following equations

$$\Psi(\mathbf{r}, t) = \langle \Psi_0(\mathbf{K}_0, \mathbf{r}) \rangle + \int d\mathbf{r}_1 G(\mathbf{r}, \mathbf{r}_1)[e\gamma\Delta V(\mathbf{r}_1, t)\langle \Psi_0(\mathbf{r}_1, t) \rangle], \quad (\text{B1})$$

$$\hat{H}_0\langle \Psi_0 \rangle = e\gamma[V'\langle \Psi_0 \rangle], \quad (\text{B2})$$

where

$$[V'\langle \Psi_0 \rangle] = e\gamma \int d\mathbf{r}_1 [G(\mathbf{r}, \mathbf{r}_1) \times \langle \Delta V(\mathbf{r}, t)\Delta V(\mathbf{r}_1, t) \rangle \langle \Psi_0(\mathbf{K}_0, \mathbf{r}_1) \rangle], \quad (\text{B3})$$

$$\hat{H}_0 G(\mathbf{r}, \mathbf{r}_1) = \delta(\mathbf{r} - \mathbf{r}_1), \quad (\text{B4})$$

and

$$\hat{H}_0 = \left(-\frac{\hbar^2}{2m_0}\nabla^2 - e\gamma V_0 - E\right). \quad (\text{B5})$$

Although some approximations were introduced in deriving Eq. (17), we now prove that the calculation based on Eqs. (B1), (B2), (B3), (B4) and (B5) (or equivalently Eqs. (17) and (22)) indeed covers exactly all orders of diffuse scattering. The current density defined in quantum mechanics is used for this proof. With consideration of diffuse scattering generated by different crystal configurations, a time and structure average is made on the current density

$$\left\langle \int_{\Sigma} d\mathbf{S} \cdot \mathbf{j}_0 \right\rangle = \frac{\hbar}{2im_0\gamma} \int_{\text{vol}} d\mathbf{r} \langle [\Psi^*\nabla^2\Psi - \Psi\nabla^2\Psi^*] \rangle, \quad (\text{B6})$$

where the integral  $\sum$  is over the crystal surface and the integral vol is over the crystal volume. From Eq. (18a)

$$H_0\Psi(\mathbf{r}, t) = e\gamma[V'\langle \Psi_0 \rangle] + e\gamma\Delta V\langle \Psi_0 \rangle, \quad (\text{B7})$$

the following calculations can be made

$$\begin{aligned} & -\frac{\hbar^2}{2m_0} \langle [\Psi^*\nabla^2\Psi - \Psi\nabla^2\Psi^*] \rangle \\ &= \langle \Psi^*H_0\Psi - \Psi H_0\Psi^* \rangle = \langle \{ \langle \Psi_0^* \rangle \\ &+ \int d\mathbf{r}_1 G^*(\mathbf{r}, \mathbf{r}_1)[e\gamma\Delta V(\mathbf{r}_1, t)\langle \Psi_0^*(\mathbf{r}_1, t) \rangle] \} \\ &\times \{ e\gamma[V'\langle \Psi_0 \rangle] + e\gamma\Delta V\langle \Psi_0 \rangle \} \rangle - \langle \{ \langle \Psi_0 \rangle \\ &+ \int d\mathbf{r}_1 G(\mathbf{r}, \mathbf{r}_1)[e\gamma\Delta V(\mathbf{r}_1, t)\langle \Psi_0(\mathbf{r}_1, t) \rangle] \} \\ &\times \{ e\gamma[V'\langle \Psi_0 \rangle]^* + e\gamma\Delta V\langle \Psi_0^* \rangle \} \rangle \\ &= e\gamma\langle \Psi_0^* \rangle [V'\langle \Psi_0 \rangle] + (e\gamma)^2 \langle \Psi_0 \rangle \int d\mathbf{r}_1 \\ &\times G^*(\mathbf{r}, \mathbf{r}_1) \langle \Delta V(\mathbf{r}, t)\Delta V(\mathbf{r}_1, t) \rangle \langle \Psi_0^*(\mathbf{r}_1, t) \rangle \\ &- e\gamma\langle \Psi_0 \rangle [V'\langle \Psi_0 \rangle]^* - (e\gamma)^2 \langle \Psi_0^* \rangle \int d\mathbf{r}_1 \\ &\times G(\mathbf{r}, \mathbf{r}_1) \langle \Delta V(\mathbf{r}, t)\Delta V(\mathbf{r}_1, t) \rangle \langle \Psi_0(\mathbf{r}_1, t) \rangle = 0, \end{aligned} \quad (\text{B8})$$

i.e.,  $\left\langle \int_{\Sigma} d\mathbf{S} \cdot \mathbf{j}_0 \right\rangle = 0$ . Therefore, the total incident

intensity equals the total out coming intensity, which means that the multiple diffuse scattering are automatically included in the calculation using Eqs. (17) and (22). Since no assumption was made in the scattering geometry of the crystal system, this conclusion is universal and is not restricted to high-energy electrons.

### Appendix C

The Green's function represents the electron wave distributed in the space due to a point source located at  $\mathbf{r}=\mathbf{r}'$  in the crystal. In this section, we use the Green's function given by Dudarev et al. [49] to calculate the optical potential for a general case. The Green's function for electron scattering has been proved to be in the form of

$$G(\mathbf{r},\mathbf{r}_1) = \frac{m_0}{2\pi^2\hbar^2} \lim_{\epsilon \rightarrow 0} \int d\kappa \frac{\exp(-2\pi i\kappa \cdot \mathbf{r}_1)}{(\kappa^2 - K_0^2 - i\epsilon)} \Psi_0^{(0)}(\kappa, \mathbf{r}). \quad (\text{C1})$$

#### Case 1: The Bloch wave approach

Take a double Fourier transform of  $G(\mathbf{r},\mathbf{r}')$

$$\hat{G}(\mathbf{u},\mathbf{v}) = \frac{m_0}{2\pi^2\hbar^2} \lim_{\epsilon \rightarrow 0} \frac{\Phi_0^{(0)}(-\mathbf{v},\mathbf{u})}{(v^2 - K_0^2 - i\epsilon)}, \quad (\text{C2})$$

where  $\Phi_0^{(0)}(\kappa,\mathbf{u})$  is the Fourier transform of  $\Psi_0^{(0)}(\kappa,\mathbf{r})$ , and the negative sign of the wave vector indicates that the incident plane wave strikes the crystal from the bottom surface. Substituting this equation into Eq. (25), the optical potential in the Bloch wave representation is

$$V'_{gh}^{(i)} = \frac{e\gamma m_0}{2\pi^2\hbar^2 V_c} \sum_j \sum_{g'} [\int d\boldsymbol{\tau}(\kappa) \alpha_j(\kappa) C_{g'}^{(j)}(\kappa) \times \frac{S(\mathbf{k}_i + \mathbf{g} - \kappa - v_j \hat{z} - \mathbf{g}', \mathbf{k}_i + \mathbf{h} - \kappa)}{\kappa^2 - K_0^2} + i \frac{\pi}{2K_0} \int d\sigma(\kappa) \alpha_j(\kappa) C_{g'}^{(j)}(\kappa) \times S(\mathbf{k}_i + \mathbf{g} - \kappa - v_j \hat{z} - \mathbf{g}', \mathbf{k}_i + \mathbf{h} - \kappa)], \quad (\text{C3})$$

where the integral  $\boldsymbol{\tau}(\kappa)$  is over all reciprocal space except a spherical shell defined by  $|\kappa|=K_0$ , the integral  $\sigma(\kappa)$  is over the Ewald sphere surface defined by  $K=K_0$ ,  $\mathbf{k}_i = \mathbf{K} + v_j \hat{z}$ , and  $C_{g'}^{(j)}(\kappa)$  are the Bloch wave coefficients of Eq. (24) without consideration of the optical potential  $V$ . The integral of  $\mathbf{u}$  is to sum over the components scattered to the entire reciprocal space. Since  $1/(\kappa^2 - K_0^2)$  is an

antisymmetric function when  $\kappa \rightarrow (K_0 - \epsilon)$  and  $\kappa \rightarrow (K_0 + \epsilon)$ , and thus the integral around the singular point  $\kappa=K_0$  is approximately zero. Thus, no abnormal numerical singularity is expected in the numerical calculation.

#### Case 2: The parallel-to-surface multi-slice approach

From Eq. (29), the solution of Eq. (10) is in the form

$$\Psi_0^{(0)}(\kappa, \mathbf{r}) = \sum_{g'} \Psi_{g'}^{(0)}(\kappa, x) \exp[2\pi i(\kappa_t + \mathbf{g}'_t) \cdot \boldsymbol{\rho}]. \quad (\text{C4})$$

Substituting Eqs. (C1) and (C4) into Eq. (31c), and performing the integrals, we obtain

$$V'_{gh}(x) = \frac{e\gamma}{S_c} \frac{m_0}{2\pi^2\hbar^2} \sum_{g'} \lim_{\epsilon \rightarrow 0} \int dQ_x \times \int d\mathbf{u} \frac{S(Q_x, \mathbf{K}_t + \mathbf{g}_t - \mathbf{u}_t - \mathbf{g}'_t, \mathbf{K}_t + \mathbf{h}_t - \mathbf{u})}{(u^2 - K_0^2 - i\epsilon)} \times \Psi_{g'}^{(0)}(\mathbf{u}, x) = \frac{e\gamma}{S_c} \frac{m_0}{2\pi^2\hbar^2} \sum_{g'} \int dQ_x [\int d\boldsymbol{\tau}(\mathbf{u}) \times \frac{S(Q_x, \mathbf{K}_t + \mathbf{g}_t - \mathbf{u}_t - \mathbf{g}'_t, \mathbf{K}_t + \mathbf{h}_t - \mathbf{u})}{(u^2 - K_0^2)} \Psi_{g'}^{(0)}(\mathbf{u}, x) + i \frac{\pi}{2K_0} \int d\sigma(\mathbf{u}) S(Q_x, \mathbf{K}_t + \mathbf{g}_t - \mathbf{u}_t - \mathbf{g}'_t, \mathbf{K}_t + \mathbf{h}_t - \mathbf{u}) \times \Psi_{g'}^{(0)}(\mathbf{u}, x)]. \quad (\text{C5})$$

If the Green's function is replaced by its form in free space

$$G_0(\mathbf{r},\mathbf{r}_1) = \frac{2m_0}{\hbar^2} \frac{\exp(2\pi i K_0 |\mathbf{r} - \mathbf{r}_1|)}{4\pi |\mathbf{r} - \mathbf{r}_1|} = \frac{m_0}{2\pi^2\hbar^2} \lim_{\epsilon \rightarrow 0} \int d\kappa \frac{\exp[2\pi i\kappa \cdot \mathbf{r} - \mathbf{r}_1]}{(\kappa^2 - K_0^2 - i\epsilon)}, \quad (\text{C6})$$

the optical potential is calculated as follows:

$$V'_{gh}(x) = \frac{e\gamma}{S_c} \frac{m_0}{2\pi^2\hbar^2} \int dQ_x \times [\int d\boldsymbol{\tau}(\mathbf{u}) \frac{S(\mathbf{K}_t + \mathbf{g}_t - \mathbf{u}_t, Q_x, \mathbf{K}_t + \mathbf{h}_t - \mathbf{u})}{(u^2 - K_0^2)}$$

$$\begin{aligned} & \times \exp(2\pi i u_x x) + i \frac{\pi}{2K_0} \int d\sigma(\mathbf{u}) \\ & \times S(\mathbf{K}_t + \mathbf{g}_t - \mathbf{u}_t, Q_x, \mathbf{K}_t + \mathbf{h}_t - \mathbf{u}) \quad (C7) \\ & \times \exp(2\pi i u_x x)]. \end{aligned}$$

Detailed calculation of Eq. (C5) has been given elsewhere [54].

## References

- [1] T. Hanada, S. Ino and H. Daimon, *Surf. Sci.* 313 (1994) 143.
- [2] J.M. McCoy, U. Korte, P.A. Makasym and G. Meyer-Ehmsen, *Phys. Rev. B* 48 (1993) 4721.
- [3] S. Schwegmann, W. Tappe and U. Korte, *Surf. Sci.* 334 (1995) 55.
- [4] H.A. Bethe, *Ann. Phys.* 87 (1928) 55.
- [5] R. Colella, *Acta Crystallogr. A* 28 (1972) 11.
- [6] A.R. Moon, *Z. Naturforsch.* 27B (1972) 390.
- [7] E.G. McRae, *Surf. Sci.* 11 (1968) 472.
- [8] P.A. Maksym and J.L. Beeby, *Surf. Sci.* 110 (1981) 423.
- [9] A. Ichimiya, *Jpn. J. Appl. Phys.* 22 (1983) 176. *Ultramicroscopy* 48 (1993) 425.
- [10] D.F. Lynch and A.F. Moodie, *Surf. Sci.* 32 (1972) 422. D.F. Lynch and A.E. Smith, *Phys. Status Solidi B* 119 (1983) 355.
- [11] A.E. Smith, G. Lehmpfuhl and Y. Uchida, *Ultramicroscopy* 41 (1992) 367. A.E. Smith and D.F. Lynch, *Acta Crystallogr. A* 44 (1988) 780.
- [12] T.C. Zhao, H.C. Poon and S.Y. Tong, *Phys. Rev. B* 38 (1988) 1172.
- [13] S.L. Dudarev and M.J. Whelan, *Surf. Sci.* 310 (1994) 373.
- [14] G. Meyer-Ehmsen, *Surf. Sci.* 219 (1989) 177.
- [15] L.M. Peng and J.M. Cowley, *Acta Crystallogr. A* 42 (1986) 545. J.M. Cowley and A.F. Moodie, *Acta Cryst.* 10 (1957) 609.
- [16] Z.L. Wang, *Reflection Electron Microscopy and Spectroscopy for Surface Analysis* (Cambridge University Press, Cambridge, 1996) chs. 3 and 9.
- [17] Z.L. Wang, *Elastic and Inelastic Scattering in Electron Diffraction and Imaging* (Plenum, New York, London, 1995) chs. 6, 7 and 10.
- [18] R. Holmestad, O.L. Krivanek, R. Høier, K. Marthinsen and J.C.H. Spence, *Ultramicroscopy* 52 (1993) 454.
- [19] Y. Horio, Y. Hashimoto, K. Shiba and A. Ichimiya, *Jpn. J. Appl. Phys.* 34 (1995) 5869.
- [20] C.C. Ahn, unpublished results.
- [21] C.B. Duke and G.E. Laramore, *Phys. Rev. B* 2 (1970) 4765.
- [22] G.E. Laramore and C.B. Duke, *Phys. Rev. B* 2 (1970) 4783.
- [23] C.B. Duke and G.E. Laramore, *Phys. Rev. B* 3 (1971) 3183.
- [24] G.E. Laramore and C.B. Duke, *Phys. Rev. B* 3 (1971) 3198.
- [25] C.B. Duke, N.O. Lipari and U. Landman, *Phys. Rev. B* 8 (1973) 2454.
- [26] C.B. Duke and U. Landman, *Phys. Rev. B* 6 (1972) 2956.
- [27] A.R. Moon, *Z. Naturforsch.* 25 A (1970) 752.
- [28] U. Korte and G. Meyer-Ehmsen, *Surf. Sci.* 298 (1993) 299.
- [29] G. Meyer-Ehmsen, B. Bölger and P.K. Larsen, *Surf. Sci.* 224 (1989) 591.
- [30] U. Korte and G. Meyer-Ehmsen, *Surf. Sci.* 277 (1992) 109.
- [31] J.L. Beeby, *Surf. Sci.* 298 (1993) 307.
- [32] S. Dudarev, L.M. Peng and M.I. Ryazanov, *Acta Crystallogr. A* 47 (1991) 170.
- [33] U. Korte and G. Meyer-Ehmsen, *Phys. Rev. B* 48 (1993) 8345.
- [34] B.A. Joyce, J.H. Neave, J. Zhang and P.J. Dobson, in: *Reflection High-Energy Electron Diffraction and Reflection Electron Imaging of Surfaces*, Eds. P.K. Larsen and P.J. Dobson (Plenum, New York, 1988) p. 397.
- [35] N.F. Mott and H.S.W. Massey, *The Theory of Atomic Collisions*, 3rd Ed. (Clarendon, Oxford, 1965), ch. 13.
- [36] S. Takagi, *J. Phys. Soc. Jpn.* 13 (1958) 278.
- [37] J.M. Cowley, *Diffraction Physics*, 3rd revised Ed. (Elsevier, Amsterdam, 1995), chs. 7 and 17.
- [38] P.H. Dederichs, *Solid State Phys.* 27 (1972) 135.
- [39] H. Yoshioka, *J. Phys. Soc. Jpn.* 12 (1957) 618.
- [40] H. Yoshioka and Y. Kainuma, *J. Phys. Soc. Jpn.* 17 (Suppl. B-II) (1962) 134–136.
- [41] S.L. Dudarev, L.M. Peng and M.J. Whelan, *Phys. Rev. B* 48 (1993) 13408.
- [42] S.L. Dudarev, L.M. Peng and M.J. Whelan, *Surf. Sci.* 279 (1992) 380.
- [43] Y. Ma, S. Lordi, C.P. Flynn and J.A. Eades, *Surf. Sci.* 302 (1994) 241.
- [44] M. Born, *Rep. Prog. Phys.* 9 (1942) 294.
- [45] S.L. Dudarev, L.M. Peng and M.J. Whelan, *Proc. R. Soc. London A* 440 (1993) 567.
- [46] B.E. Warren, *X-Ray Diffraction* (Dover, New York, 1990) ch. 11.
- [47] Z.L. Wang, *Acta Crystallogr. A* 51 (1995) 569.
- [48] P.A. Flinn, *Phys. Rev.* 104 (1956) 350.
- [49] S.L. Dudarev, D.D. Vvedensky and M.J. Whelan, *Phys. Rev. B* 50 (1994) 14525.
- [50] J.M. Cowley, *J. Appl. Phys.* 21 (1950) 24.
- [51] C.R. Hall, *Philos. Mag.* 12 (1965) 815.
- [52] Z.L. Wang, *Acta Crystallogr. A*, in press.
- [53] Z.L. Wang, *Philos. Mag. B*, in press.  
Z.L. Wang, *Scanning Microsc.* (1997), to be published.